Co-Crystal Formation of Partially Fluorinated 1,3,5-Tris(phenylethynyl)benzenes

Jan-Henrik Weddeling, Paul Lukas Waltersmann, Beate Neumann, Hans-Georg Stammler, and Norbert W. Mitzel*[a]

Several rigid 1,3,5-tris(phenylethynyl)benzenes with different fluorination patterns were synthesized through selective Sonogashira-Hagihara coupling reactions to analyze the packing behavior in solid-state structures. The aggregation is dominated by various intermolecular interactions between aryl substituents, triple bonds, C–H bonds and H···F contacts. Co-crystallization experiments for the analysis of preferred aryl-aryl-interactions led to 1:1 complexes. Intermolecular phenyl-perfluorophenyl interactions with short centroid-centroid distances are dominating these co-crystal structures. They lead to melting point increases of up to 49 °C for the co-crystals compared to the pure substances.

1. Introduction

Rigid organic frameworks linked by aryl-alkynyl backbones and efficient π-delocalization are used in many fields of chemistry. Applications for 1,3,5-triethynylbenzene (TEB) include building blocks for light emitting diodes (LED),[1] non-linear optics (NLO)[2] or macromolecules,[3] the synthesis of tridentate Lewis acids[4] as well as the formation of columnar supramolecular solids.[5] All these studies are focusing on the molecular shape and electronic characteristics of the TEB backbone. Non-covalent interactions of the backbone were not yet highlighted in these studies.

Over the past years, intermolecular stacking interactions between arenes and perfluoroarenes, especially the solid-state structures of benzene and hexafluorobenzene (HFB), received significant attention.[6] As pure substances, both aggregate in herringbone-like structures in their crystal lattices.[7] In contrast, an equimolar mixture of benzene and HFB crystallizes in an alternating array featuring both molecules in a parallel displaced structure.[8] These intermolecular stacking interactions increase the melting point by about 18 °C relative to the pure substances.[9] This phenomenon was first observed by Patrick and Prosser in 1960.[8] Recent studies pointed out that the interaction energy is significantly composed of London dispersion forces,[10] the attractive part of van-der-Waals interactions.[11] To analyze this stacking behavior, different aromatic groups were linked with rigid or flexible backbones.[12,13–15] A few literature examples deal with the stacking effects of molecules with alkynyl-linked phenyl/perfluorophenyl groups and demonstrate their use for preordering in solid or liquid phases.[16–18]

In this work, we aim at combining the rigid backbone of C_3-symmetric TEB with the strong interactions between benzene and perfluorobenzene groups as a driving force for the aggregation of molecules in an attempt of crystal engineering. The preparation of molecules with different fluorination patterns and the investigations of their solid-state structures demonstrate these aggregation processes, in order to help controlling crystallization.

2. Results and Discussion

2.1. Syntheses

For the syntheses of triethynylbenzenes (TEBs) **1**–**8** (Figure 1), we used the Sonogashira-Hagihara coupling reactions starting from the aryl halides.[19] Fluorinated building blocks for coupling reactions can be prepared in a facile and economic access, the iodation of fluorobenzenes. We used a modified protocol of Wenk et al. to synthesize 1,3,5-triiodo-2,4,6-trifluorobenzene (90% yield).[20] TEBs **5**–**8**, featuring a fluorinated core, were synthesized starting from 1,3,5-triiodo-2,4,6-trifluorobenzene. For the syntheses of 1,3,5-triethynylbenzenes **1**–**4** we used commercially available 1,3,5-tribromobenzene. Depending on the coupling partners for Sonogashira-Hagihara coupling reactions, the experimental conditions had to be modified.[21] We decided to use a co-catalyst system consisting of copper(I) iodide and a palladium(0) species, $[Pd(PPh_3)_4]$.

Tetrakis(triphenylphosphane)palladium (**$[Pd(PPh_3)_4]$**) is on the one hand more selective for coupling reactions, but on the other hand more expensive and more sensitive towards oxygen and moisture than the analogous palladium(II) species $[Pd(PPh_3)_2Cl_2]$ which is also frequently employed in coupling reactions. We decided to use catalyst **A** and diisopropylamine

[a] Dr. J.-H. Weddeling, P. L. Waltersmann, B. Neumann, Dr. H.-G. Stammler, Prof. Dr. N. W. Mitzel
Lehrstuhl für Anorganische Chemie und Strukturchemie, Centrum für Molekulare Materialien CM$_2$,
Fakultät für Chemie, Universität Bielefeld
Universitätsstraße 25, 33615 Bielefeld (Germany)
E-mail: mitzel@uni-bielefeld.de

Supporting information for this article is available on the WWW under https://doi.org/10.1002/open.202100194

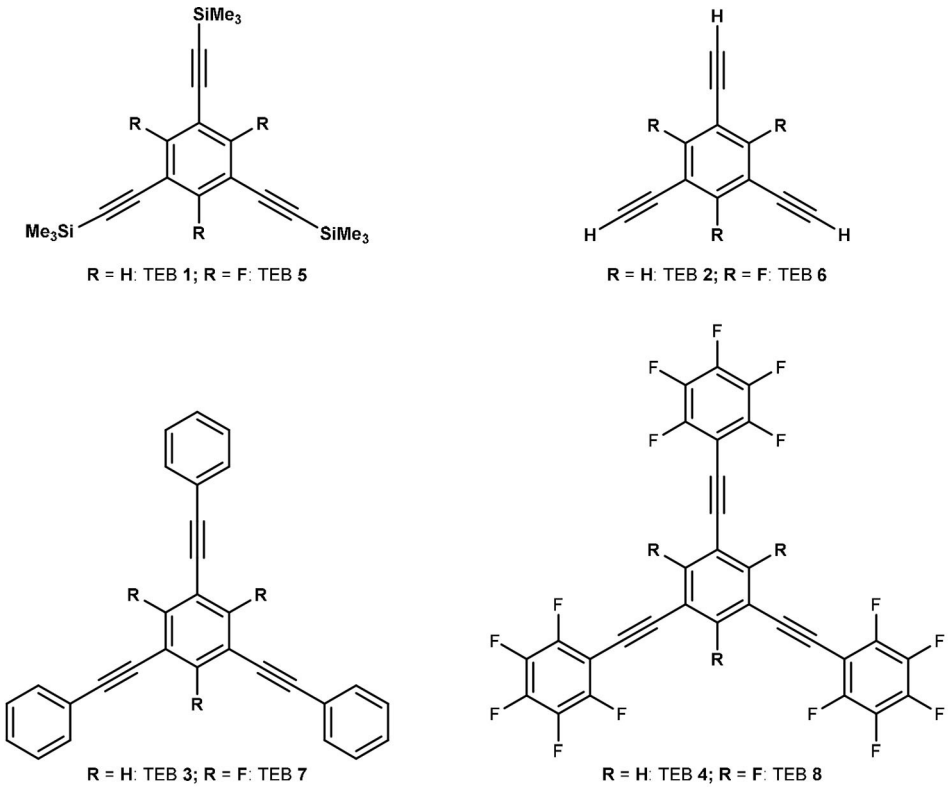

Figure 1. Substitution pattern of 1,3,5-triethynylbenzenes (TEBs) **1**–**8**.

as solvent and base and added tetrahydrofuran in cases of limited solubility of the compounds. After aqueous workup, all coupling reactions afforded acceptable to good yields (Table 1). Our chosen conditions led to higher yields for compounds **1**, **3** and **4**.[22,24,25] For TEBs with a fluorinated core, catalyst **B** [$Pd(PPh_3)_2Cl_2$] resulted in higher yields.[25] Compound **8**, which is fluorinated both central and radial, had not been documented in literature before.

2.2. Structural Analysis in the Solid State

Although 1,3,5-triethynylbenzenes (TEBs) have been known for many years and have many applications, some of the crystal structures had not yet been available. Herein we report the so far not described solid-state structures (TEBs **1**, **6**, **7**, **8**) and compare their structural parameters with those of literature-known structures to analyze the packing behavior (Table 2).

Table 1. Isolated and literature yields.

Compound	R	R′	Yield [%]	Literature Yield [%]
1	H	TMS	80	74[22]
2	H	H	90	92[23] [a]
3	H	Ph	97	82[24]
4	H	Ph_F	38	30[16]
5	F	TMS	42	69[25] [b]
6	F	H	34	46[25] [a]
7	F	Ph	28	71[25] [b]
8	F	Ph_F	27	[c]

[a] Authors used different deprotection method; [b] authors used catalyst **B** [c] compound is unknown in literature.

1,3,5-Tris(trimethylsilylethynyl)benzene (TEB **1**) crystallizes in the orthorhombic space group *Pbca* (Figure 2). In the crystal lattice, its molecules arrange in parallel stacks with long distances between their centroids within the stack [7.908(1) Å]. One of the trimethylethynyl units of TEB **1** is directed into the neighboring stack, leading to σ-π-interactions between a methyl group and the benzene core of the neighboring molecule. The distance between the carbon atom of the methyl group and the centroid of the benzene core is 3.847(2) Å. On the opposite side of the core, a corresponding and slightly longer contact of 3.929(2) Å is present. Fourmigué et al. determined the crystal structure of the fluorinated analogue **5**;[28] it crystallizes in a structure of parallel sheets and is dominated by multiple intermolecular H···F-contacts [2.58(1) Å H(7)···F(1)] between the fluorinated benzene core and the methyl groups of the terminal TMS groups.

The crystal structures of TEBs **2**–**4** and **6**–**8** (Figures 3 and 4) show a different aggregation motif. In their crystal lattices, the molecules arrange in parallel displaced structures with short intermolecular contacts between aryl groups and the neighboring C≡C triple bonds.[18,26,27] The resulting distances are given in Table 2.

Compound **6** crystallizes in the monoclinic space group $P2_1/c$. The molecules in the crystal lattice arrange in an offset orientation with an intermolecular centroid-centroid distance of

Table 2. Structural parameters of compounds **1**–**8**. Listed distances (< 5 Å) represent the shortest observed intermolecular distances.

	R = H				R = F			
R′ =	–TMS	–H	–Ph	–Ph_F	–TMS	–H	–Ph	–Ph_F
Compound	1	2	3	4	5	6	7	8
Reference	[a]	[26]	[27]	[16]	[28]	[a]	[a]	[a]
Space group	*Pbca*	*C*2/c	$P2_1/c$	$P2_1/c$	$P31_C$	$P2_1/c$	$P2_1/c$	$P2_1/c$
R [%]	3.37	5.83	7.65	7.49	4.71	4.70	3.75	3.45
θ $Ph_{(centl)}$–$Ph_{(rad)}$ [°]	–	–	0.4, 8.6, 80.5	4.1, 27.8, 89.9	–	–	9.0(1), 13.3(1), 70.6(1)	3.5(1), 3.8(1), 6.5(1)
$d_{centr\text{-}centr}$ [Å]	–	3.947(2)	4.857(1)	5.001(1)	–	4.826(1)	5.001(1)	5.023(1)
$d_{centr\text{–}C\equiv C}$ [Å] [b]	–	3.833(4), 4.553(3), 4.525(3)	3.497(7), 3.377(7), 4.747(7), 4.769(7)	3.395(8), 3.444(8), 4.241(8), 3.535(8)	–	3.373(1), 4.867(1), 4.743(1)	3.537(1), 3.616(1), 4.125(1), 4.243(1)	3.855(1), 3.894(1), 3.613(1), 3.616(1)
$d_{C\text{–}C}$ [Å]	3.629(2) (C4···C18)	3.508(4) (C5···C11)	3.420(10) (C2···C23)	3.418(14) (C16···C20)	3.340(5) (C8···C9)	3.433(2) (C1···C4)	3.433(2) (C1···C4)	3.244(2) (C6···C24)

[a] This work; [b] distance between the centroid of the aryl group and the centroid of the C–C-triple bond.

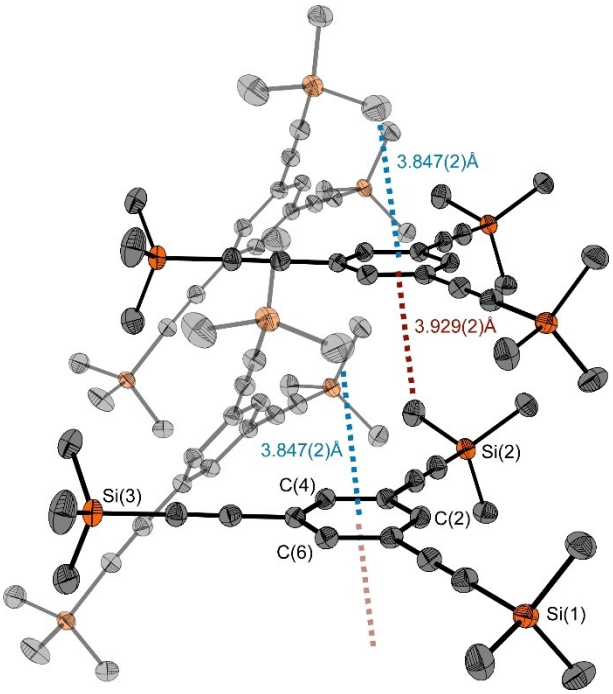

Figure 2. Molecular structure and aggregation of **1** in the crystalline state with an intermolecular centroid-C_{CH3} distance of 3.847(2) Å ($^1/_2$–*x*, $^1/_2$+*y*, +*z*). Displacement ellipsoids are drawn at the 50% probability level. Hydrogen atoms are omitted for clarity. Interlocking molecules from the neighboring stack are drawn at 50% transparency level. Symmetry operation for generating equivalent positions: +*x*, −1+*y*, +*z*.

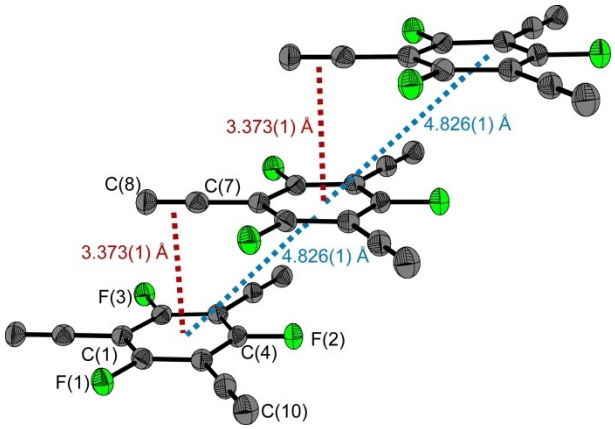

Figure 3. Molecular structure and aggregation of **6** in the crystalline state with an intermolecular centroid-centroid distance (blue) of 4.826(1) Å and a centroid-triple bond distance (red) of 3.373(1) Å. Displacement ellipsoids are drawn at the 50% probability level. Hydrogen atoms are omitted for clarity. Symmetry operation for generating equivalent positions: −1+*x*, +*y*, +*z* and 1+x, +y, +z.

4.826(1) Å and receive additional stabilization through an intermolecular H···F contact between neighboring columns. Interestingly, the triple bond sits right atop the neighboring benzene ring in central orientation with a centroid-triple bond distance of 3.373(1) Å. This sandwich-like arrangement relative to the neighboring counterpart is unique among the 1,3,5-triethynylbenzenes **1**–**8** and the aryl-triple bond distance is the shortest observed for those molecules.

Terminally arylated TEBs show a similar aggregation behavior. Compound **7** shows at least four contacts between triple bonds and neighboring aryl groups (Figure 4b) with intermolecular distances around 4 Å. The centroid-centroid distances between neighboring molecules in the crystal lattice [5.001(1) Å] are too long for an aryl-aryl-interaction.

For terminally aryl-substituted TEBs (**3**, **4**, **7**, **8**) a different structural parameter appears to influence aggregation in the solid. The electrostatic repulsion of the terminal phenyl groups causes distortion and twisting along the acetylene bridge, leading to a propeller-type structure (except for TEB **8**). The interplanar twist angle θ between the central benzene unit and the terminal aryl systems indicates how much these molecular parts are twisted. The electrostatic repulsion of the aryl groups seems to modify the planar star-shaped structure into a propeller form. Interplanar angles (θ) between the central and radial benzene rings are 0.2(3)–89.9(3)° and the acetylene bonds are slightly bent (174–178°; Ø = 178°). This phenomenon was also observed in the earlier reported solid-state structures of compound **3** and **4**.[16,27] The newly investigated TEB **8**, fluorinated at the central and radial benzene rings, shows a different solid-state structure. Whereas the centroid-centroid and centroid-triple bond distances are comparable to TEBs **3**, **4** and **7**

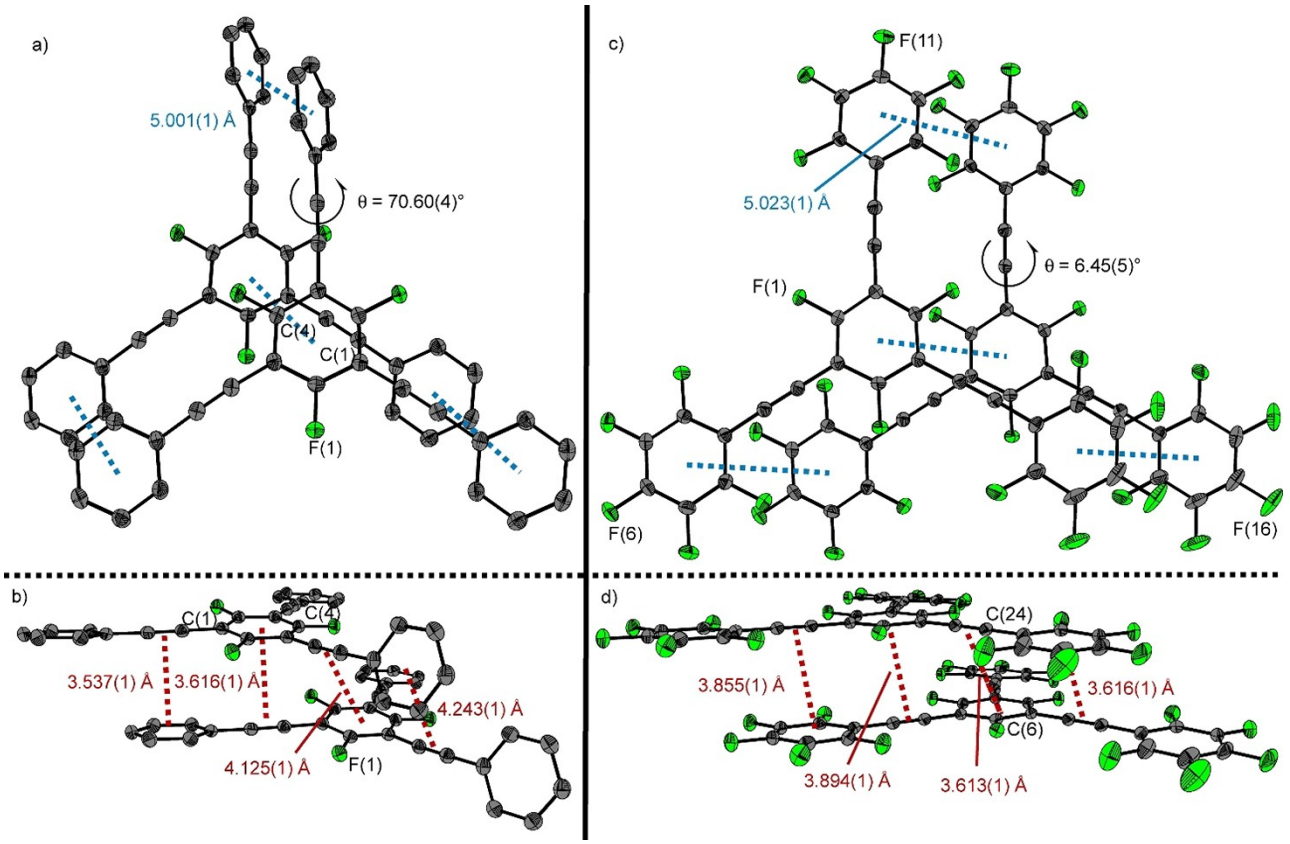

Figure 4. Molecular structure and aggregation of **7** and **8** in the crystalline state. Displacement ellipsoids are drawn at 50% probability level. Hydrogen atoms are omitted for clarity. Top view (a, c): intermolecular centroid-centroid distance (blue) and interplanar twist angles θ. Side on view (b, d): centroid-centroid (triple bond, mean plane) distances (red). Symmetry operation for generating stacks ($+x$, $1+y$, $+z$) and equivalent positions: **7**: $+x$, $-1+y$, $+z$; **8**: $+x$, $-1+y$, $+z$.

(Table 2), the interplanar angles between the central and radial benzene rings are significantly smaller [$\theta = 3.5(1)°$, 3.8(1)° and 6.5(1)°]. The nearly co-planar terminal perfluorophenyl groups lead to a star-shaped structure. The propeller form caused by the electrostatic repulsion is not favored.

The herein reported solid-state structures of pure 1,3,5-triethynylbenzenes show different aggregation motifs of their molecular constituents. Whereas the packing behavior of compounds **1** and **5** is dominated by interactions of the terminal trimethylsilyl groups with the neighboring stack in the crystal lattice, the terminally arylated TEBs **3**, **4**, **7** and **8** are stabilized by a mixture of intermolecular aryl-aryl and aryl-acetylene contacts. The inter-planar twist angles between terminal and central aryl rings reach up to 90°. Intermolecular phenyl-pentafluorophenyl interactions as a packing motif were not observed for the partially fluorinated compounds **4** and **7**. In order to evaluate the influence of such heteroaryl-aryl-interactions, we investigated the formation and structure of co-crystals.

2.3. Co-Crystallization Experiments

From our experience with inter- and intramolecular stacking interactions between phenyl and perfluorophenyl groups in partially fluorinated linked bis-arenes, we knew that such interactions have a striking impact on the aggregation behavior in the solid-state but also on the conformational behavior in the gas-phase.[13–15] Siegel et al. already investigated the structures of TEBs **3** and **4**, as well as the corresponding co-crystal (**Co II**) of both.[16] Inspired by this work, we investigated the co-crystallization behavior of the terminally arylated TEBs. All possible combinations were attempted to be realized, but only the successful experiments are reported here. Table 3 lists

Table 3. Co-crystallization experiments for TEBs **3**, **4**, **7** and **8**.

Complex	Combination ring substituent inner	outer	Component 1		Component 2	
Co I	H·F	H·H	3	$C_6H_3(CC{-}C_6H_5)_3$	7	$C_6F_3(CC{-}C_6H_5)_3$
Co II [a]	H·H	H·F	3	$C_6H_3(CC{-}C_6H_5)_3$	4	$C_6H_3(CC{-}C_6F_5)_3$
Co III	F·H	H·F	7	$C_6F_3(CC{-}C_6H_5)_3$	4	$C_6H_3(CC{-}C_6F_5)_3$
Co IV	H·F	H·F	3	$C_6H_3(CC{-}C_6H_5)_3$	8	$C_6F_3(CC{-}C_6F_5)_3$

[a] Co-crystal was examined by Siegel *et al.*[16]

the different combinations of TEB species. First, we investigated the influence of the fluorination pattern on the aggregation motifs in the co-crystals. Subsequently, the macroscopic stability of the co-crystals, in comparison to their individual pure substances, was checked by determining their melting points.

In order to learn more about the aryl-aryl interactions at the central and terminal benzene units of the 1,3,5-triethynylbenzenes, we attempted to evaluate the individual contributions by combining the co-crystal constituents systematically: only one position in the fluorination pattern of the used TEBs was changed from system to system (see Table 3).

First, we investigated the aryl-aryl interaction at the central benzene unit by varying the respective TEBs only at the central position in their fluorination pattern. The structure of Siegel's **Co II** was used to study the interactions between terminal aryl groups. Finally, two combinations (**Co III**, **Co IV**) of TEBs that differ in their fluorination pattern both terminally and centrally were investigated. The generation of the co-crystalline specimens was achieved by slowly evaporating hexane/dichloromethane-solutions of equimolar amounts of the respective compounds. The resulting crystals were picked and investigated by X-ray diffraction.

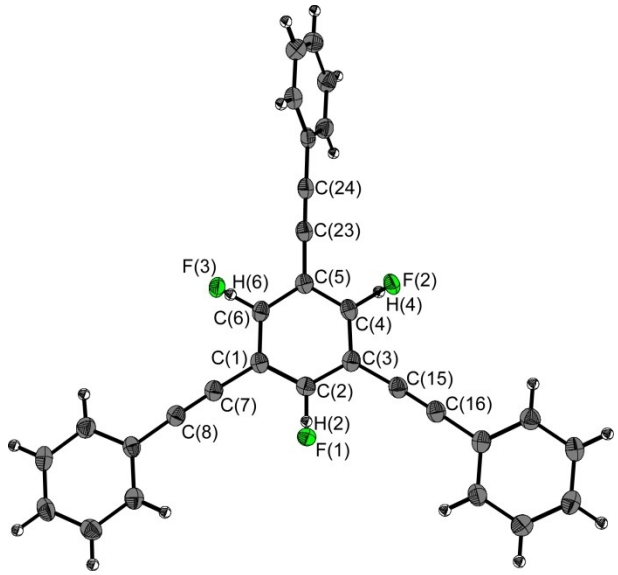

Figure 5. Molecular structure of **Co I** in the crystalline state. Displacement ellipsoids are drawn at the 50% probability level. TEB **3** and TEB **7** share the same site with an 86:14 distribution. Symmetry operation for generating equivalent positions: $+x$, $-1+y$, $+z$.

With the first co-crystal (**Co I**), we intended to investigate the influence of an aryl-perfluoroaryl interaction at the central benzene unit. Co-crystal **Co I** (Figure 5) crystallizes in the same space group ($P2_1/c$) and is isostructural to the crystal structure of pure TEB **7** (Figure 4). In the crystal lattice of **Co I**, molecules of TEBs **3** and **7** share the same place, building a mixed crystal. The occupation sites in **Co I** are not occupied in an alternating sequence of both co-crystal constituents, but instead are statistically distributed with a ratio of 86:14 (TEB **3**: TEB **7**). The structural parameters of **Co I** (Table 4) are nearly identical to that of TEB **7**. Due to the statistical distribution, it is not possible to derive clear information on the influence of the fluorination pattern on the aggregation in the solid. The stacks are formed along the *b*-axis (like for TEB **7**) with nearly identical centroid-centroid distance [4.993(1) Å]. However, because of the almost identical aggregation behavior in relation to the structure of pure TEB **7**, it can be assumed that there is no significantly stronger attractive interaction and *vice versa* no influence to the aggregation in solid.

Table 4 contains structural parameters of Siegel's **Co II**. The observed co-crystal had a remarkably changed packing behavior in contrast to corresponding pure TEBs or **Co I**. The alternating stacks, formed by TEBs **3** and **4**, aggregate in a sandwich orientation and the molecules within the column are essentially planar. In contrast to crystal structures of pure TEBs **3** and **4**, the centroid-centroid distances of 3.654(4)–4.034(4) Å are decreased and indicate intermolecular aryl-aryl-interactions between phenyl and pentafluorophenyl groups.

Both **Co III** and **Co IV** (Figure 6) crystallized in columnar stacks with alternating molecules of the corresponding TEBs. Whereas aryl-triple bond contacts are negligible, the columnar packing behavior in the crystal lattice is comparable to the

Table 4. Structural parameters of co-crystals **Co I**–**Co IV**. Shown distances (< 5 Å) are the shortest observed intermolecular distances.

	Co I	Co II [a]	Co III	Co IV
Space group	$P2_1/c$	$P\bar{1}$	$P\bar{1}$	$P2_1/n$
R [%]	3.68	5.84	5.04	7.56
Θ $Ph_{(central)}$–$Ph_{(radial)}$ [°]	8.7(1), 13.2(1), 70.7(1)	2.5, 3.0, 9.9, 5.4, 5.8, 8.9	1.7(1), 2.5(1), 5.3(1), 4.2(1), 5.4(1), 7.2(1)	5.6(2), 13.1(2), 23.4(2), 3.2(2), 10.6(2), 23.9(2)
$d_{centr\text{-}centr}$(central) [Å]	4.993(1)	3.827(3); 3.765(3)	3.715(1); 3.700(1)	3.729(2); 3.788(2)
$d_{centr\text{-}centr}$(radial) [Å]	4.993(1)	A: 3.654(4); 4.034(4) B: 3.706(5); 3.879(5) C: 3.794(4); 3.815(4)	A: 3.693(1); 3.730(1) B: 3.730(1); 3.693(1) C: 3.540(1); 3.942(1)	A: 3.739(3); 3.778(3) B: 3.773(3); 3.744(3) C: 3.713(2); 3.806(2)
$d_{centr\text{-}C\equiv C}$ [Å] [b]	3.537(1), 3.616(1), 4.129(1), 4.236(1)	A: 4.050(5) B: 4.862(6) C: 4.189(6)	A: 4.393(1) B: 4.070(1) C: 4.090(1)	A: 4.008(2) B: 3.917(2) C: 4.956(2)
$d_{C\text{-}C}$ [Å]	3.531(2) (C5···C7)	3.437(9) (C18···C39)	3.313(2) (C18···C47)	3.392(6) (C16···C47; C30···C55)

[a] Solid-state structure was determined by Siegel *et al.*;[16] [b] distance between the centroid of the aryl group and the centroid of the C–C-triple bond.

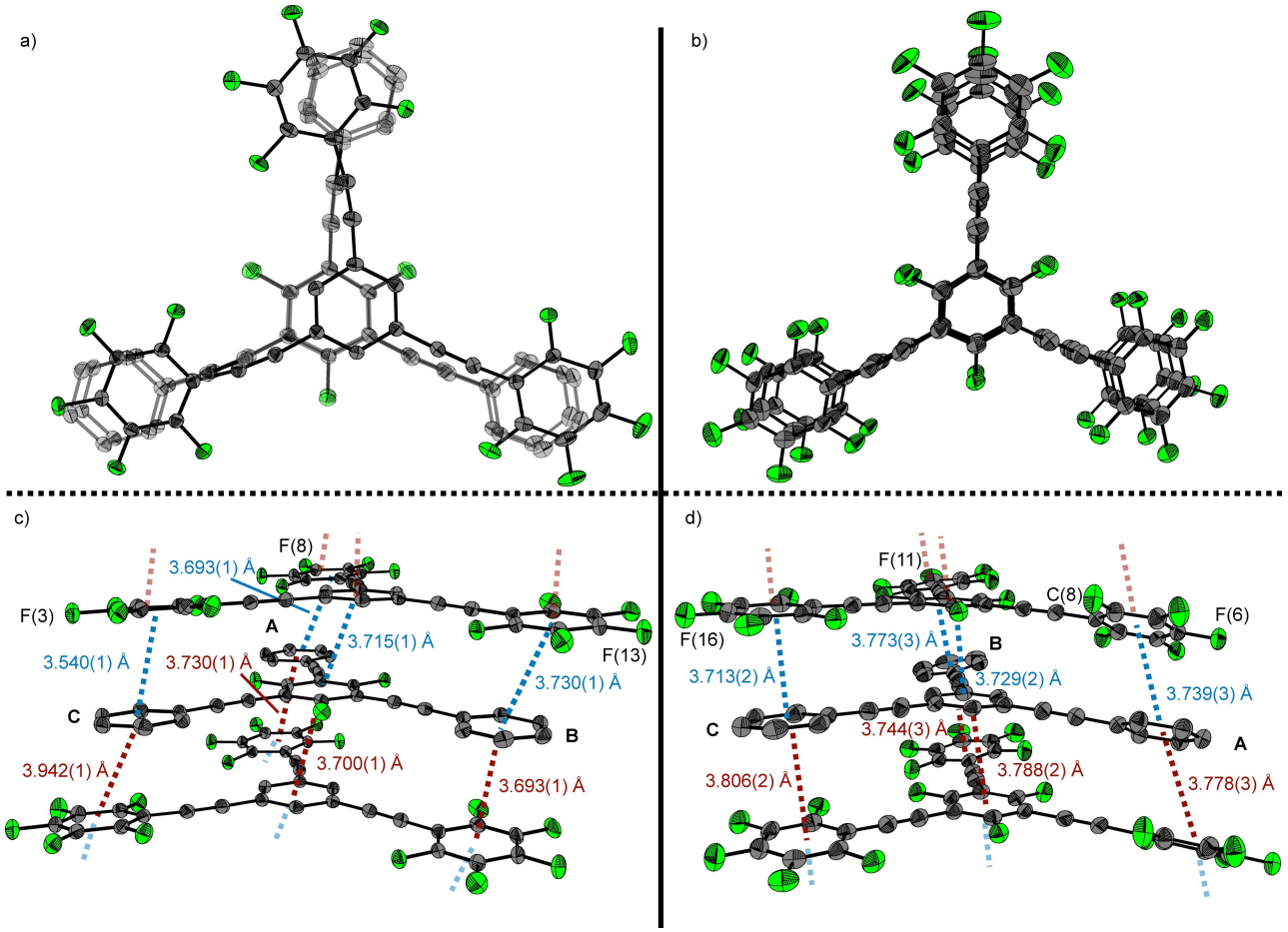

Figure 6. Molecular structure and aggregation of **Co III** and **Co IV** in the crystalline state. Displacement ellipsoids are drawn at the 50% probability level. Hydrogen atoms are omitted for clarity. (a, b) Top view with stacking of both components along the *a*-axis. (c, d) Side view with eight independent intermolecular aryl-aryl-interactions to neighboring molecules (**A**, **B**, **C**, **central**) with corresponding centroid-centroid distances. Symmetry operations for generating equivalent positions for **Co III** and **Co IV**: $-1+x, +y, +z$.

solid-state structure of **Co II**. The packing in the crystal lattice of **Co IV** is slightly more ordered compared to **Co III** (see Figures 6a, 6c). The arrangement of columns in the structure of **Co III** is promoted by intercolumnar H···F contacts [for example 2.53(2) Å H(42) ···F(15), 2.59(2) Å H(50)···F(7), 2.56(2) Å H(49)···F(8)] and also the benefit of maximum packing density. In contrast to **Co I**, we found eight independent centroid-centroid distances [3.540(1)–3.942(1) Å] between the aryl groups in each site of crystal lattice in **Co III**, which are slightly shorter than for **Co II**, but significantly shorter than for the pure TEBs **1**–**8** (Table 2). The parallel arrangement in displaced order is nearly congruent, with small slip angles about 20° (sandwich: 0°, off-stacked: 45°). The propeller form is not favored for **Co III** and **Co IV**; instead, the molecules are essentially planar. With **Co IV**, we investigated the combination of the fluorinated TEB **10** and the pure hydrocarbon TEB **3**. For this co-crystal, we expected a planar alignment of the terminal aryl groups, because the molecular structure of pure TEB **8** in the solid state is essentially planar (Figure 4d). In order to prepare **Co IV**, hexane/dichloromethane-solutions of equimolar amounts of both constituents were combined, resulting in an instantaneous precipitation of a colorless, non-crystalline solid. This solid could not be dissolved again in these solvents, even by heating and ultrasonication. A crystallization from hot toluene finally afforded needle-shaped crystals. After examination of a large number of crystals from different crystallization experiments, a solid-state structure of **Co IV** could finally be determined. We found a columnar structure (Figure 6b) of alternating molecules of TEBs **3** and **8** with eight independent centroid distances [3.713(3)–3.806(2) Å]. The expected coplanarity, initiated by a pre-organization of TEB **8**, was not observed; instead, the interplanar twist angles found in the co-crystal are quite large [$\theta = 5.6(2)°$, 13.1(2)°, 23.4(2)°, 3.2(2)°, 10.6(2)°and 23.9(2)°].

Based on the analysis of the obtained co-crystals, we were able to draw conclusions on the relationship between the fluorination motif and the aggregation behavior of the used TEBs. Differentiation of the fluorination pattern only at the central benzene unit (**Co I**) did not lead to significantly changed aggregation motifs compared to pure substances. The combination of TEBs with different fluorination patterns at the terminal aryl groups (**Co II**) led to highly ordered columnar structures. By analyzing the solid structures of co-crystals **Co II**–**IV**, we found aryl-aryl interactions between fluorinated and non-fluorinated aryl groups with short intermolecular centroid-

centroid distances. The additional aryl interactions between the central benzene (**Co III**, **Co IV**) units do not significantly alter the packing behavior.

In order to see if the aryl-aryl interactions influence the macroscopic stability, we analyzed the melting points of pure substances and co-crystals (see Table 5 for melting points of the co-crystals and corresponding TEBs). These results clearly demonstrate the influence of aryl-aryl-interactions of fluorinated and non-fluorinated aryl groups on the stabilization of solid-state structures. The difference was determined by using the melting point of the co-crystal and the highest melting point of the pure compounds, respectively. The difference is up to 49 °C (**Co IV**) and shows the strong influence of the aryl-aryl interaction between fluorinated and non-fluorinated aromatic groups of the studied TEBs. A direct relationship between the melting point difference and the number of aryl-aryl interactions, centroid distances or the planarity of the molecules in the solid could not be established. However, it could be shown that the strong influence of the investigated interactions influenced the stacking behavior in the solid-state and the melting point of the resulting co-crystals. The combination of a rigid backbone and precisely tuned substituents leads to aggregation in the solid-state, which could be used for a wide range of applications depending on the composition of the individual TEBs.

Further co-crystallization studies were undertaken, inspired by Gabbaï's columnar supramolecular solid.[5] Therefore, we slowly evaporated THF solutions of equimolar amounts of TEBs **1**–**8** and $[o\text{-}C_6F_4Hg]_3$ and analyzed the resulting crystals with X-ray diffraction. We were able to examine a co-crystal **Co V**, which showed the formation of columnar stacks of alternating entities of TEB **3** and $[o\text{-}C_6F_4Hg]_3$ (see Figures S32 and S33, Supporting Information). Within the stacks, the interplanar distances and distances between the Hg atoms to the neighboring TEB **3** in the crystal lattice are slightly shorter than for Gabbaï's co-crystal and are given in detail in the Supporting Information.

3. Conclusion

The solid-state structures of 1,3,5-triethynylbenzenes (TEB) show aggregation motifs depending on their substitution patterns. While the packing behavior of compounds with terminal trimethylsilyl groups is dominated by intermolecular σ-π interactions and H···F contacts to neighboring molecules in the crystal lattice, the aggregation of terminally arylated TEBs is dominated by a combination of intermolecular aryl-aryl and aryl-acetylene contacts. Depending on the fluorination pattern, the planarity and rigidity of the backbone can be modified. In order to analyze intermolecular interactions between fluorinated and non-fluorinated aryl groups, we investigated a series of co-crystals of two different TEBs. The differentiation of the fluorination pattern at the terminal aryl groups led to alternating columnar structures in the solid state. Melting point analyses of the co-crystals showed the striking impact of phenyl-perfluorophenyl interactions on the stabilization in the solid state by increasing the melting points by 34–49 °C in contrast to the pure co-crystal constituents. These investigations of solid-state structures of modified 1,3,5-triethynylbenzenes could lead to applications in molecular recognition processes, reversible surface loading and crystal engineering.

Deposition Number(s) 2036255 (for 1), 2036256 (for 6), 2036257 (for 7), 2036258 (for 8) contain the supplementary crystallographic data for this paper. These data are provided free of charge by the joint Cambridge Crystallographic Data Centre and Fachinformationszentrum Karlsruhe Access Structures service.

Table 5. Melting points of pure compounds and co-crystals.[a]

Compound a Mp. [°C]	Compound b Mp. [°C]	Co-Crystal Mp. [°C]	Difference[a] ΔT [K]
144 (TEB 3)	201 (TEB 4)	239 (Co II)[b]	38
197 (TEB 7)	201 (TEB 4)	235 (Co III)	34
144 (TEB 3)	245 (TEB 8)	294 (Co IV)	49

[a] Difference to highest melting pure compound; [b] melting point was determined by Siegel et al.[16]

Acknowledgements

We thank Klaus-Peter Mester and Marco Wißbrock for recording NMR spectra and Barbara Teichner for elemental analyses. This work was funded by DFG (German Research Foundation) in the Priority Program SPP1807 "Control of LD in molecular chemistry" (grant MI477/28-2, project no. 271386299).

Conflict of Interest

The authors declare no conflict of interest.

Keywords: 1,3,5-triethynylbenzene · crystal engineering · halogenated arenes · phenyl-perfluorophenyl interactions · solid-state structures

[1] F. Wang, B. R. Kaafarani, D. C. Neckers, *Macromolecules* **2003**, *36*, 8225–8230.
[2] I. R. Whittall, M. G. Humphrey, S. Houbrechts, J. Maes, A. Persoons, S. Schmid, D. C. R. Hockless, *J. Organomet. Chem.* **1997**, *544*, 277–283.
[3] J. M. Tour, *Chem. Rev.* **1996**, *96*, 537–554.
[4] A. Schwartzen, L. Siebe, J. Schwabedissen, B. Neumann, H.-G. Stammler, N. W. Mitzel, *Eur. J. Inorg. Chem.* **2018**, *2018*, 2533–2540.
[5] T. J. Taylor, V. I. Bakhmutov, F. P. Gabbaï, *Angew. Chem. Int. Ed.* **2006**, *45*, 7030–7033; *Angew. Chem.* **2006**, *118*, 7188–7191.
[6] J. C. Collings, K. P. Roscoe, E. G. Robins, A. S. Batsanov, L. M. Stimson, J. A. K. Howard, S. J. Clark, T. B. Marder, *New J. Chem.* **2002**, *26*, 1740–1746.
[7] a) N. Boden, P. P. Davis, C. H. Stam, G. A. Wesselink, *Mol. Phys.* **1973**, *25*, 81–86; b) E. G. Cox, D. W. J. Cruickshank, J. A. S. Smith, *Proc. R. Soc. London Ser. A* **1958**, *247*, 1–21; c) J. H. Williams, J. K. Cockcroft, A. N. Fitch, *Angew. Chem. Int. Ed. Engl.* **1992**, *31*, 1655–1657.
[8] C. R. Patrick, G. S. Prosser, *Nature* **1960**, *187*, 1021.
[9] J. H. Williams, *Acc. Chem. Res.* **1993**, *26*, 593–598.

[10] a) B. W. Gung, J. C. Amicangelo, *J. Org. Chem.* **2006**, *71*, 9261–9270; b) S. Tsuzuki, T. Uchimaru, M. Mikami, *J. Phys. Chem. A* **2006**, *110*, 2027–2033; c) M. O. Sinnokrot, C. D. Sherrill, *J. Am. Chem. Soc.* **2004**, *126*, 7690–7697.
[11] a) F. London, *Z. Phys.* **1930**, *63*, 245–279; b) F. London, *Trans. Faraday Soc.* **1937**, *33*, 8b.
[12] a) A. S. Shetty, J. Zhang, J. S. Moore, *J. Am. Chem. Soc.* **1996**, *118*, 1019–1027; b) M. L. Renak, G. P. Bartholomew, S. Wang, P. J. Ricatto, R. J. Lachicotte, G. C. Bazan, *J. Am. Chem. Soc.* **1999**, *121*, 7787–7799; c) F. Cozzi, F. Ponzini, R. Annunziata, M. Cinquini, J. S. Siegel, *Angew. Chem. Int. Ed. Engl.* **1995**, *34*, 1019–1020; d) F. Cozzi, J. S. Siegel, *Pure Appl. Chem.* **1995**, *67*, 683–689; e) M. Linnemannstöns, J. Schwabedissen, B. Neumann, H.-G. Stammler, R. J. F. Berger, N. W. Mitzel, *Chem. Eur. J.* **2020**, *26*, 2169–2173.
[13] S. Blomeyer, M. Linnemannstöns, J. H. Nissen, J. Paulus, B. Neumann, H.-G. Stammler, N. W. Mitzel, *Angew. Chem. Int. Ed. Engl.* **2017**, *56*, 13259–13263.
[14] M. Linnemannstöns, J. Schwabedissen, A. A. Schultz, B. Neumann, H.-G. Stammler, R. J. F. Berger, N. W. Mitzel, *Chem. Commun.* **2020**, *56*, 2252–2255.
[15] J.-H. Weddeling, Y. Vishnevskiy, B. Neumann, H.-G. Stammler, N. W. Mitzel, *Chem. Eur. J.* **2020**.
[16] F. Ponzini, R. Zagha, K. Hardcastle, J. S. Siegel, *Angew. Chem. Int. Ed. Engl.* **2000**, *39*, 2323–2325.
[17] a) J. Kendall, R. McDonald, M. J. Ferguson, R. R. Tykwinski, *Org. Lett.* **2008**, *10*, 2163–2166; b) G. W. Coates, A. R. Dunn, L. M. Henling, D. A. Dougherty, R. H. Grubbs, *Angew. Chem. Int. Ed. Engl.* **1997**, *36*, 248–251.
[18] F. Ponzini, R. Zagha, K. Hardcastle, J. S. Siegel, *Angew. Chem. Int. Ed.* **2000**, *39*, 2323–2325; *Angew. Chem.* **2000**, *112*, 2413–2415.
[19] a) K. Sonogashira, Y. Tohda, N. Hagihara, *Tetrahedron Lett.* **1975**, *16*, 4467–4470; b) S. Takahashi, Y. Kuroyama, K. Sonogashira, N. Hagihara, *Synthesis* **1980**, *1980*, 627–630.
[20] H. H. Wenk, W. Sander, *Eur. J. Org. Chem.* **2002**, *2002*, 3927–3935.
[21] K. Sonogashira, *J. Organomet. Chem.* **2002**, *653*, 46–49.
[22] S. Leininger, P. J. Stang, S. Huang, *Organometallics* **1998**, *17*, 3981–3987.
[23] A. Carpita, L. Mannocci, R. Rossi, *Eur. J. Org. Chem.* **2005**, *2005*, 1859–1864.
[24] Z. Ruan, W. Rong, Q. Li, Z. Li, *Carbon* **2015**, *87*, 338–346.
[25] G. Hennrich, A. M. Echavarren, *Tetrahedron Lett.* **2004**, *45*, 1147–1149.
[26] H.-C. Weiss, D. Bläser, R. Boese, B. M. Doughan, M. M. Haley, *Chem. Commun.* **1997**, 1703–1704.
[27] M. N. Bochkarev, M. A. Katkova, E. A. Fedorova, N. P. Makarenko, H. Schumann, F. Girgsdies, *Z. Naturforsch.* **1998**, *53b*, 833–835.
[28] J. Lieffrig, O. Jeannin, M. Fourmigué, *J. Am. Chem. Soc.* **2013**, *135*, 6200–6210.

Manuscript received: August 16, 2021
Revised manuscript received: September 22, 2021